



Research Article

# Preparation of Bi<sub>2</sub>O<sub>3</sub>/TiO<sub>2</sub>-Montmorillonite Nanocomposites and Their Applications to the Photodegradation of Pentachlorophenol

Nacéra Boumahdi<sup>1</sup>, Amel Hadj-Ziane-Zafour<sup>1,\*</sup>, Hafsa Yaiche-Achour<sup>2,3</sup>, Hussein Khalaf<sup>1</sup>

<sup>1</sup>Laboratoire de Génie Chimique (LGC), Faculté de Technologie, Université Blida 1, B.P 270, Route de Soumaa, 09000 Blida, Algeria.

<sup>2</sup>Laboratoire de Biologie des Systèmes Microbiens (LBSM), Ecole Normale Supérieure de Kouba, Alger, Algeria.

<sup>3</sup>Ecole Supérieure des Sciences de l'Aliment et des Industries Agroalimentaires, Beau Lieu, El Harrach Alger, Algeria.

Received: 2<sup>nd</sup> October 2021; Revised: 18<sup>th</sup> November 2021; Accepted: 19<sup>th</sup> November 2021

Available online: 22<sup>nd</sup> November 2021; Published regularly: March 2022



## Abstract

In the past decades, there has been a growing tendency to study the different techniques that can increase the photocatalytic efficiency as well as recyclability of new products “photocatalysts” for water treatment. In this last research the effect of bismuth addition to titanium was investigated. Bi/Ti-pillared montmorillonites have been prepared from natural Algerian bentonite exactly from deposits of Maghnia situated in the west side of the country. These nanocomposites were characterized by X-ray diffraction (XRD), Brunauer-Emmet-Teller (BET), scanning electron microscopy (SEM) methods, and Fourier Transformed Infrared (FT-IR). The photocatalytic activities have been tested for the removal of pentachlorophenol (PCP) in water. The effect of preparation conditions, the pH of the solution and photocatalysts concentration, on these activities has been investigated. It was found that the photocatalytic degradation increase by addition of bismuth in pillaring process. The Mont-Bi-Ti is shown to be the best photocatalyst in term of photocatalytic activity.

Copyright © 2021 by Authors, Published by BCREC Group. This is an open access article under the CC BY-SA License (<https://creativecommons.org/licenses/by-sa/4.0>).

**Keywords:** Bi<sub>2</sub>O<sub>3</sub>; TiO<sub>2</sub>; Montmorillonite; Nanocomposites; Pentachlorophenol; Photocatalysis

**How to Cite:** N. Boumahdi, A. Hadj-Ziane-Zafour, H. Yaiche-Achour, H. Khalaf (2022). Preparation of Bi<sub>2</sub>O<sub>3</sub>/TiO<sub>2</sub>-Montmorillonite Nanocomposites and Their Applications to the Photodegradation of Pentachlorophenol. *Bulletin of Chemical Reaction Engineering & Catalysis*, 17(1), 78-87 (doi: 10.9767/bcrec.17.1.12421.78-87)

**Permalink/DOI:** <https://doi.org/10.9767/bcrec.17.1.12421.78-87>

## 1. Introduction

Chlorophenols have the ability to bioaccumulate in organisms, alongside potential mutagenic and carcinogenic effects. More over these products change the quality of drinking water. For this reasons, they are listed as a first pollutants in most water regulation authorities [1].

Pentachlorophenol (PCP) is a highly chlorinated hydrocarbon more used as bactericide, insecticide, herbicide and wood preservative. This compound is carcinogenic and harmful to plants, human and animals even at weak concentrations [2,3]. PCP is known as an environmental precursor for the formation of polychlorinated dibenzo-*p*-dioxins (PCDDs) and polychlorinated dibenzofurans (PCDFs), which are seriously toxic [3]. PCP is also known as getting a high level of toxicity, that's why conventional water and

\* Corresponding Author.

Email: [amelzafour@yahoo.fr](mailto:amelzafour@yahoo.fr) (A. Hadj-Ziane-Zafour);  
Telp: +213 5 53860933

waste water treatment technologies can't remove chlorophenols when dissolved in aqueous systems [1].

The heterogeneous photocatalytic oxidation is one of the very promising technologies, based on the total mineralization of dangerous organic compounds that are so difficult to be degraded [4]. As one of the most successful methods, photocatalysis attracted increasing environmental and energy concerns. Among known photocatalysts, titanium dioxide ( $\text{TiO}_2$ ) is used as an important semiconductor material with a lot desirable properties, like the absence of toxicity, exceptional physical and chemical stability, and low cost. Even though it has well known performances and stabilities,  $\text{TiO}_2$  based photocatalysts present limited applications due the wide bandgap energy (3.2 eV) and high recombination rate. To enhance photocatalytic activity of  $\text{TiO}_2$ , a lot of ways were widely used and developed; like the ones which include doping various ions into  $\text{TiO}_2$  lattice, sensitization by using absorbed molecules [5]. The enhancement of photocatalytic activities can be achieved mainly by decreasing the particle size of photocatalysts down to nanoparticles, development and optimization of binary semiconductors nanostructured materials and reducing the global process cost requires, avoiding microfiltration by immobilizing the semiconductor catalyst on a support [4].

Earlier studies indicate that clay supported semiconductor nanocomposites are found to be a promising technique for wastewater treatment. It improves photocatalytic activity as it provides larger surface area, basal space and cation exchange capacity. Montmorillonite is abundant and low cost clay. It is effectively combined with different semiconductors to form composites for its adsorption desorption property [6]. The progress realized in clay pillaring method by several metallic species points to the application of semiconductor-pillared clays as photocatalysts. The intercalated semiconductors in the interlayer spaces of clays, in the form of nanosize pillars could enhance its photocatalytic activity. In addition, the high adsorption capacity of clay and its high surface area could also facilitate the retention of the pollutants and their intermediate products of photocatalytic degradation. Meshram *et al.* [7] reported removal of phenol, Riaz *et al.* [8] studied the removal of orange G and Hamane *et al.* [9] focus on the removal of  $\text{Pb}^{+2}$ , using different bentonite based composites.

Different methods have been adopted to enhance  $\text{TiO}_2$  photocatalytic efficiency, like ion doping [10], dye-sensitization [11], polymer-

sensitization and doping with junction semiconductors [12-18]. However, these doping processes change other physical properties such as the lifetime of  $e^-$ - $h^+$  pairs, adsorption characteristics and photoelectrochemical stability.  $\text{Bi}_2\text{O}_3$  is an important non-toxic narrow band gap photosensitizer with a direct band gap of 2.1–2.8 eV, and its capacity of oxidation by electron holes of  $\text{Bi}_2\text{O}_3$  is considered as an important condition for a kind of good photocatalytic materials [19]. But the photocatalytic activity of  $\text{Bi}_2\text{O}_3$  is low due to the photocorrosion and fast recombination of photogenerated electron-hole pairs. In current years, the development of  $\text{Bi}_2\text{O}_3$ - $\text{TiO}_2$  composite photocatalyst that can work effectively under visible light irradiation with photochemical stability is a very important topic in photocatalysis research [20]. Therefore, many works were done in this subject [20–24].

In the present study we have developed the photocatalytic activity of nanocomposites  $\text{Bi}_2\text{O}_3/\text{TiO}_2$ -pillared montmorillonite, characterized by X-ray diffraction (XRD), scanning electron microscopy (SEM), Brunauer-Emmett-Teller methods (BET), and Fourier transform infrared (FTIR). The photocatalytic activity of these nanocomposites is tested by the photocatalytic degradation of PCP. The influence of various parameters as well a catalyst concentration and pH has been studied.

## 2. Materials and Methods

### 2.1 Synthesis Procedure

The pillared montmorillonite clays were prepared using bentonite from deposits of Maghnia in Western Algeria. According to a previously reported procedure [25], the purified raw bentonite was dispersed in 1 M NaCl, separated from the solution and washed with water to obtain a constant conductivity. The resulting suspension was placed in a graduate cylinder for allowing particles  $>2 \mu\text{m}$  in size to settle down. The suspension at the depth of 10 cm containing only particles of size  $<2 \mu\text{m}$  was collected with a Robinson-Kohn pipette. This operation was repeated several times until the suspension became almost transparent at the depth of 10 cm. Particles of a size  $<2 \mu\text{m}$  were recovered by centrifugation, washed with water and dialyzed to eliminate chloride ions in excess and finally dried at  $40^\circ\text{C}$  for 72 h. The  $\text{TiO}_2$  pillaring solution is prepared by using the sol-gel method, where a colloidal solution was prepared by the addition of Titanium tetra isopropoxide [ $\text{Ti}(\text{C}_3\text{H}_7\text{O}_2)_4$ ] and 1 N HCl, with a molar ratio  $[\text{HCl}]/[\text{Ti}] = 4$ . The mixture was

stirred for 3 h at room temperature which was washed by distilled water, centrifuged and dried at 40 °C for 72 h. Finally, the modified clay was calcined during 15 min in a microwave apparatus at 800 W [25–28]. The photocatalyst obtained was named Mont-TiO<sub>2</sub>. In a synthesis procedure, 0.1 g of Cetyltrimethylammonium Bromide (CTAB) was dissolved in 15 mL of absolute ethanol under vigorous stirring at room temperature. Then the resulting solution was ultrasonicated for 15 min before mixing with 6 mL of Ti (C<sub>3</sub>H<sub>4</sub>O<sub>2</sub>)<sub>4</sub>. After 20 min of ultrasonication, a homogeneous solution was formed and subsequently heated to 82 °C. At this time, a certain amount of bismuth(III) nitrate pentahydrate [Bi(NO<sub>3</sub>)<sub>3</sub>·5H<sub>2</sub>O] with 0.0175 of Bi/Ti (atomic ratio) was added into the solution with vigorous stirring, a yellowish sol was obtained after 30 min of ultrasonication and 180 min stirring [20]. An amount of 1 g of Mont was dispersed into 100 mL of water with vigorous stirring for 18 h to obtain 1.0% (mass) Mont dispersion. The Bi-Ti pillaring solution was added dropwise to this dispersion, with vigorous stirring, for 24 h, to have Bi-Ti-Mont. The resulting mixture was centrifuged and washed several times with water. The solid product was dried at 120 °C for 30 min and calcinated at 420 °C in a microwave, since this procedure is known to lead to photocatalytic materials with higher activity than that obtained by conventional heating [4,26,27]. In our process, it was necessary to add CTAB as the surface dispersant to make bismuth (III) nitrate pentahydrate evenly and stably suspended in ethanol to form uniform suspensions.

## 2.2 Nanocomposites Characterization

The crystal phase of the resulting material is determined by powder X-ray Diffraction (XRD) (Philips) with X'pert Pro PAN analytical polycrystalline diffractometer X'celerator RTMS detector. Fourier Transformed Infrared (FT-IR) spectra were recorded with Shimadzu model 8900 spectrophotometer using a KBr pellet technique for solid samples in the range of 4000 to 400 cm<sup>-1</sup>. A scanning electron microscopy (SEM) model JEOL JSM-6360L, controlled by a computer, was used to detect samples morphology. The measurement of the specific surface was made according to the method BET (Brunauer, Emmet and Teller), by adsorbing liquid nitrogen at 77.3 K, and by using a Quantachrome ASiQwin Automated Gas Sorption.

## 2.3 Photocatalytic Activity

To study the adsorption of PCP on the prepared nanocomposites samples, the PCP (10 mg/L) solution is magnetically stirred with nanocomposites samples in dark for 60 min to ensure adsorption–desorption equilibrium between the PCP and nanocomposites. Then changes in concentration of PCP are determined by UV–Visible spectrophotometry at the maximum wavelength of the absorption  $\lambda_{\max} = 214$  nm. The photocatalytic activity of the prepared nanocomposites samples were evaluated by the decomposition of PCP. Each photocatalyst was mixed with PCP solution. Total volume of the aqueous solution for the photocatalytic reaction was 20 mL, and the concentration of PCP was 10 mg/L, and 2.5 g/L of photocatalytic sample was suspended in this solution. The prepared solution was then irradiated by UV lamp (Philips HPK brand lamp) with 125 W power, the theoretical energy of the lamp being 47 W/m<sup>2</sup>. Cooling water jacket is used to maintain temperature inside the reactor. At given intervals of illumination, the suspension was centrifuged and then filtered through a millipore filter. The filtrates were analyzed by UV-Visible spectrophotometry.

## 3. Results and Discussion

### 3.1 Characterization of the Photocatalysts

#### 3.1.1 BET analysis

The specific surface area of samples was determined by the Nitrogen adsorption-desorption isotherms. The isotherms were analyzed by the BET method. The surface area of the Mont-Na is 87 m<sup>2</sup>/g, which increase to 128

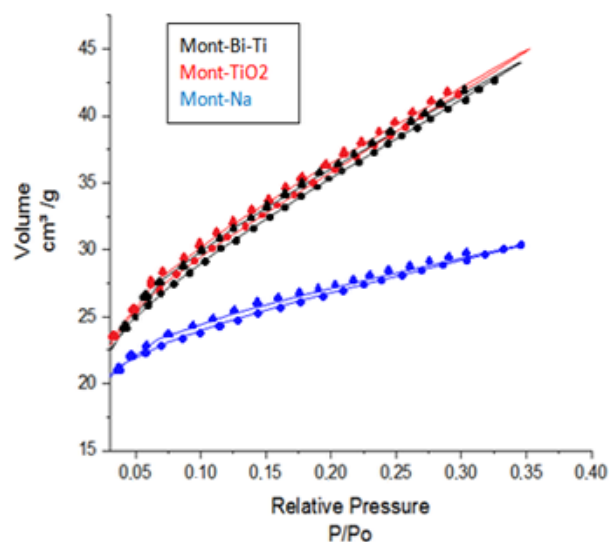


Figure 1. Isotherms of the prepared samples.

m<sup>2</sup>/g for Mont-Bi-Ti and to 129 m<sup>2</sup>/g for Mont-TiO<sub>2</sub>. An increase in the BET surface area is observed between the nanocomposites samples is due essentially to an increase of the microporosity as indicated by the modification of the shape of N<sub>2</sub> adsorption isotherm. The nitrogen adsorption-desorption isotherms for the samples are presented in Figure 1. The samples show the isotherm of type IV (BDDT classification) [29]. At high relative pressure, the isotherms of Mont-Na, Mont-TiO<sub>2</sub> and Mont-Bi-Ti exhibit hysteresis loops of type H3, this indicates that the powders contained mesopores.

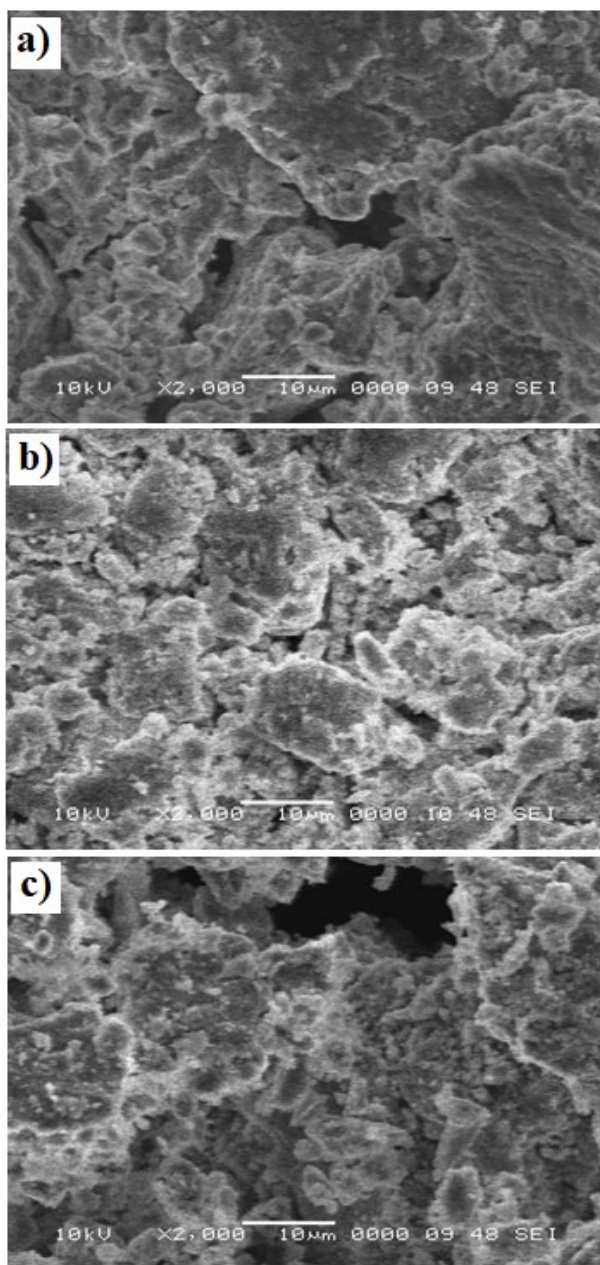


Figure 2. SEM images of (a) Mont-Na, (b) Mont-TiO<sub>2</sub> and (c) Mont-Bi-Ti.

### 3.1.2 SEM analysis

Figure 2 shows scanning electron microscopy of the prepared samples, Mont-Na, Mont-TiO<sub>2</sub> and Mont-Bi-Ti. The morphologies of prepared samples are quite similar. The shape of montmorillonite particles does not change upon introduction of the sensitizing material, suggesting that TiO<sub>2</sub> and Bi<sub>2</sub>O<sub>3</sub> deposition do not alter the montmorillonite structure. The same observations have been made by other researchers [30-33].

### 3.1.3 XRD analysis

X-ray powder diffraction is a useful tool to characterize the phase structure of the materials. The X-ray diffraction pattern of Mont-Na, Mont-TiO<sub>2</sub> and Mont-Bi-Ti are shown in Figure 3. For the purified montmorillonite, the peak at 2θ = 6.9° corresponds to a basal distance *d*<sub>001</sub> of 12.8 Å in agreement with what is well established for sodic montmorillonite [25,31,32].

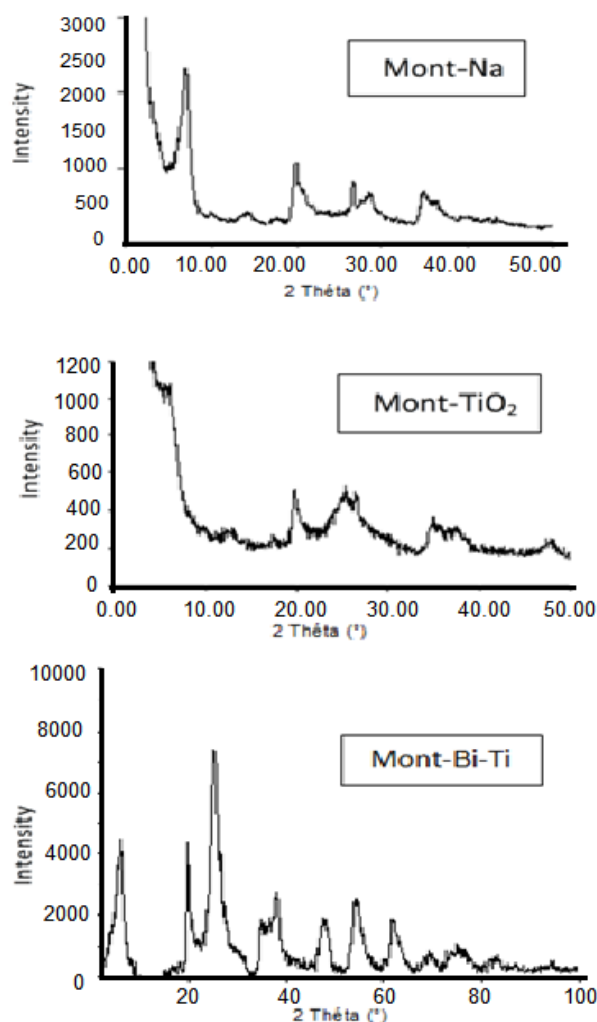


Figure 3. XRD patterns of Mont-Na, Mont-TiO<sub>2</sub> and Mont-Bi-Ti.

This result indicates the presence of a single water layer in the interlayer space of montmorillonite [34]. The diffraction pattern of Mont-TiO<sub>2</sub> shows a diffraction line  $d_{001}$  at  $2\theta = 5.05^\circ$  indicating the formation of titanium pillars as corresponding to an increase of the basal distance to 17.48 Å, while the pattern of Mont-Bi-Ti shows a (001) peak at  $2\theta = 6.57^\circ$  ( $d = 13.44$  Å) due to intercalation of polycations species of titanium and bismuth. This change indicates an increase in the basal spacing  $d$  (001). These results reveal that the pillared clays samples have good ordered layers structure with insertion of titania and bismuth pillars, which causes an increase in the clay basal spacing [4].

### 3.1.4 FT-IR analysis

Figure 4 shows the FT-IR spectra of the Mont-Na, Mont-TiO<sub>2</sub>, and Mont-Bi-Ti nanocomposites, the band observed at 3625.92 cm<sup>-1</sup> is attributed to the stretching vibrations of hydroxyl groups of the octahedral layer linked to 2 Al. the band around 3448 cm<sup>-1</sup> is due to the stretching vibrations of the OH groups of water. The observed peak band at 2364.57 cm<sup>-1</sup> is attributed to O-H from H<sub>2</sub>O and CO<sub>2</sub> adsorbed on the surface grains while handling the sample under room atmosphere [30–35]. The absorption peak at 1631 cm<sup>-1</sup> is attributed to OH deformation of water interlayer [30]. The intense band around 1037 cm<sup>-1</sup> is due to the stretching vibrations of Si-O characteristic of aluminosilicates. The peak observed at 918 cm<sup>-1</sup> is due to the hydroxide (OH) deformations linked to Al and/or Mg ions [36]. Also, the peak in 520 and 466 cm<sup>-1</sup> are related to the stretching vibrations of tetrahedral atoms in montmorillonite. The FTIR spectra reveal that the as-prepared Mont-Na, Mont-TiO<sub>2</sub> and Mont-Bi-Ti samples present the same absorption bands as the clay reference, indicating that the montmorillonite structure remained almost unchanged after treatment. This result is in good agreement with previous observations [30–35].

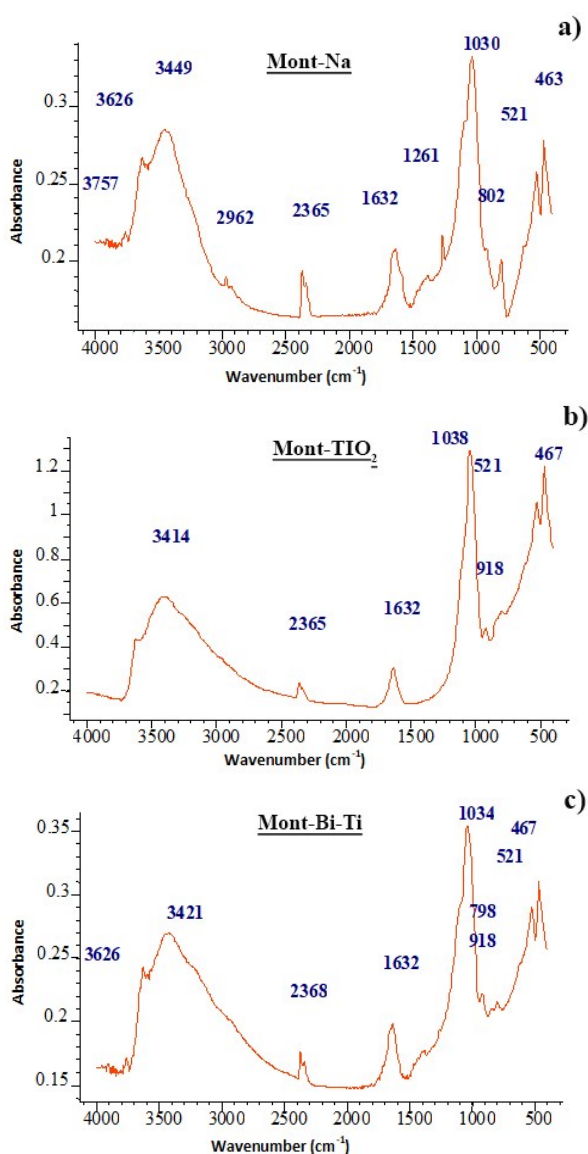


Figure 4. FTIR spectra of a) Mont-Na, b) Mont-TiO<sub>2</sub> and c) Mont-Bi-Ti.

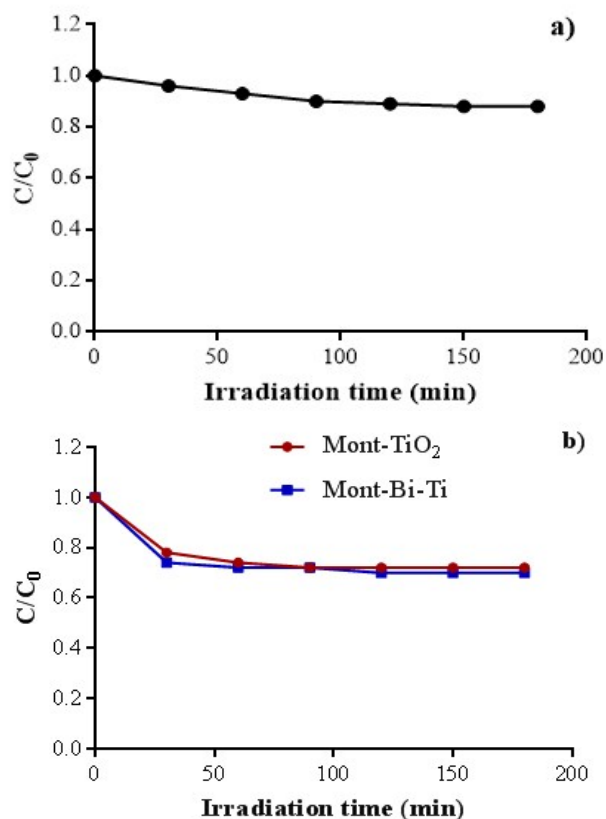


Figure 5. a) PCP photolysis and b) Adsorption of PCP with Mont-TiO<sub>2</sub> and Mont-Bi-Ti.

## 3.2 Photocatalytic Activity

Figure 5(a) illustrates the PCP photolysis. The photolysis test without nanocomposites showed that less than 4% of PCP was decomposed after 3 h of irradiation. Before each experiment, the PCP and catalyst solutions were first stirred for 1 h in the dark to reach an adsorption–desorption equilibrium. Khalfaoui-Boutoumi *et al.* and Dubey *et al.* [12,37] reported that the adsorption of organic pollutants on the surface of photocatalyst is helpful to prevent the recombination of photoinduced electron and hole.

The optimum weight of catalyst is an important parameter to be investigated to avoid ineffective excess of catalyst and to ensure the total absorption of efficient photons. To study the effect of catalyst loading on PCP degradation, experiments were conducted with different catalyst loadings: 1, 1.5, and 2.5 g/L at 10 mg/L initial PCP concentration, at solution pH = 6.86. Figure 6 show the influence of the Mont-TiO<sub>2</sub> and Mont-Bi-Ti concentration on the

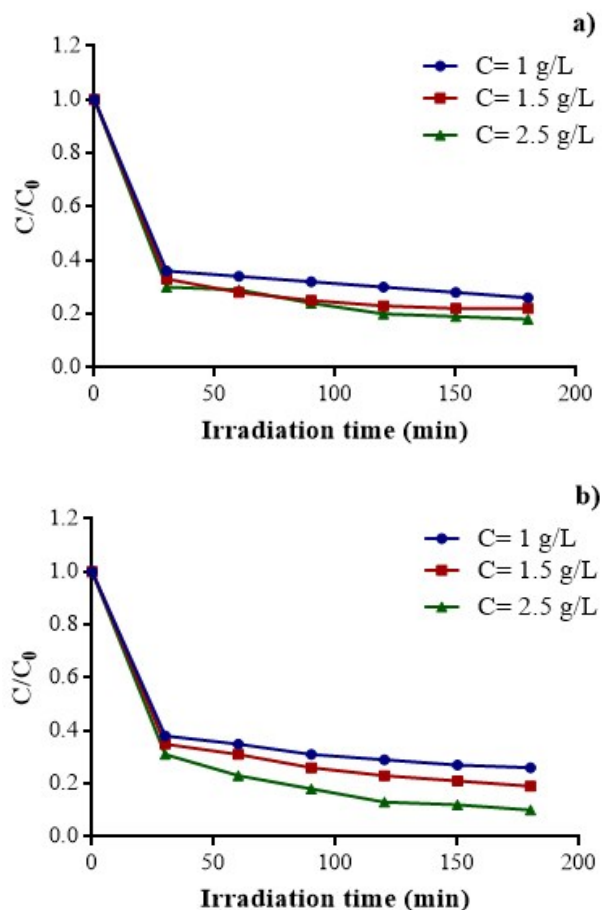


Figure 6. Photocatalytic degradation of PCP, with a) Mont-TiO<sub>2</sub> and b) Mont-Bi-Ti, depending on catalyst concentration.

photocatalytic activity by following the reduction of PCP concentration in aqueous media. The experimental results indicated that the activity increased from 69 to 76% for Mont-TiO<sub>2</sub> and 76 to 78% for Mont-Bi-Ti. This increase might be explained by the reduction of the electron-hole pair recombination rate. The Bi ions can play the role of electron acceptors. Hence, photogenerated electrons and holes would be more efficiently separated. Results indicate clearly that the presence of both synthesized photocatalyst and UV light irradiation is indispensable for PCP degradation. The Bi ions in the Mont-Bi-Ti may act as an electron trap or may increase the band gap, which resulted in the decrease in the recombination rate of photogenerated electron–hole pairs under UV light irradiation. The enhancement in photocatalytic activity of Mont-Bi-Ti can also be due to the enhanced charge transfer efficiency of Mont-Bi-Ti. The increase in surface area increases the number of active sites, which in turn promotes the separation efficiency of the electron–hole pairs resulting in enhanced photocatalytic activity (Figure 7) [38]. According to the obtained results, the amount of catalyst was kept constant at 2.5 g/L in all the rest of photocatalysis experiments.

The pH value of the solution has a relevant effect on the photocatalytic reaction because the photocatalyst surface state of protonation, its potential of zero charge, and the dissociation of PCP are all strongly pH dependent. Surface charge promotes or inhibits coulombic interactions during adsorption, thus favouring inhibiting the interaction between catalyst and pollutant, something well-known for a variety of photocatalysts [30,39–41].

In this work, pH was varied in the range (3–6.86) with initial PCP concentration of 10 mg/L and 2.5 g/L of Mont-TiO<sub>2</sub> and Mont-Bi-Ti cata-

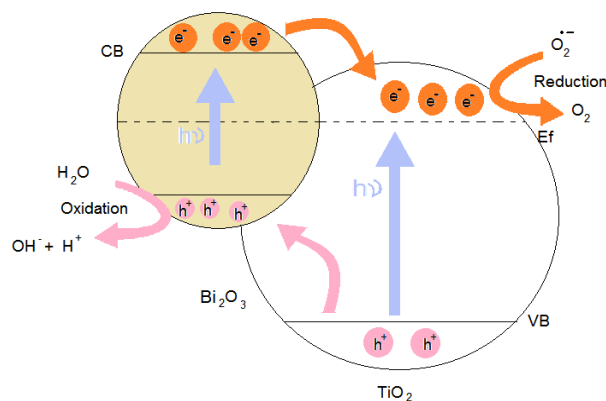


Figure 7. Photocatalytic degradation mechanism over Bi<sub>2</sub>O<sub>3</sub>/TiO<sub>2</sub> composite.

lyst load, to study its effect. As shown in Figure 8(a-b) the efficiency of the photocatalytic degradation of PCP depends on the acidity of the medium pH. PCP removal is better at acidic pH= 3 with a removal percentage around 84% after 200 min. As pH increases, the extent of removal decreases, with a reduction up to 78% at pH= 6.86. A similar observation has been reported by Pelentridou *et al.* [42] on the effect of pH on the photodegradation of the herbicide azimsulfuron and also by Dougna *et al.* [37] on phenol removal by photocatalysis. This result can be explained by the repulsion forces between the catalyst surface charge and the charge of pollutants molecules.

Indeed, the pHPzc of TiO<sub>2</sub> is about 6.8 [43] and the pKa of the pentachlorophenol is 4.75. The presumably positively charged acidic media (pH < 6.8) and negatively charged basic media (pH > 6.8) will promote or inhibit the establishment of Coulomb electrostatic strength during adsorption and can thus influence the interaction between the catalyst and the pollutant surfaces [40].

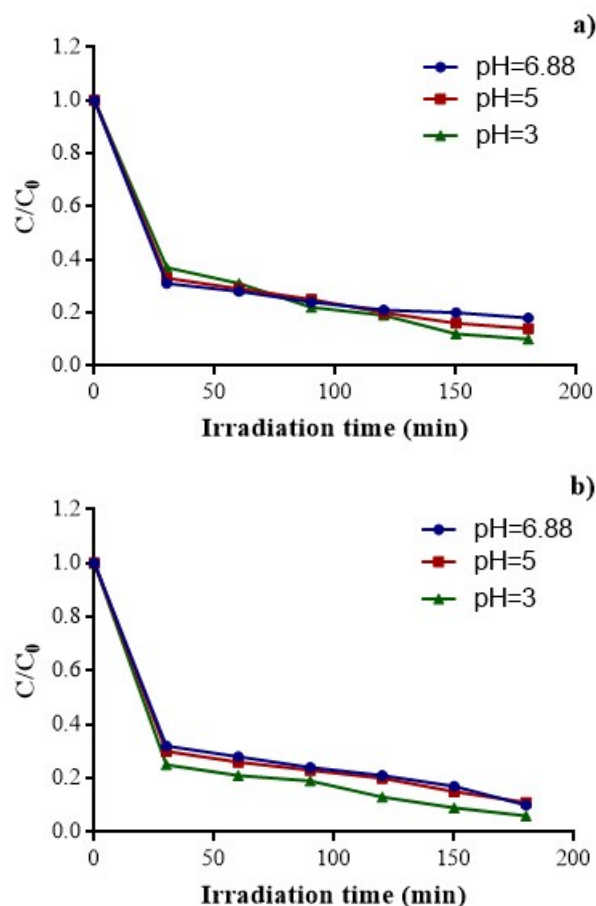


Figure 8. Photocatalytic degradation of PCP, with a) Mont-TiO<sub>2</sub> and b) Mont-Bi-Ti, depending on pH variation.

It is assumed that the surface of Bi<sub>2</sub>O<sub>3</sub>/TiO<sub>2</sub> catalyst is positively charged in acidic solution while negatively charged in alkaline solution [44]. Also, the pentachlorophenol is known as an organic substance that has a negative charge (Figure 9). Therefore, it is clear why the highest degradation is obtained at acidic pH compared to alkaline pH. The activity of the catalysts may be due to the presence of a strong electrostatic field between the surface of the positively charged catalyst and the negatively charged pollutant.

Another reason for the increase in degradation in an acidic medium is the production of hydroxyl radicals, which were higher than in an alkaline medium, so these radicals can increase the oxidation potential. In addition, the oxidation potential due to the recombination of hydroxyl radicals in an acidic medium is lower than that of an alkaline [45]. At low pH, the adsorption of cationic organic molecules on the photocatalyst surface increases, because the photocatalyst surface has a positive charge, which leads to increased adsorption of cationic organic molecules. Therefore, the degradation efficiency increases at low pH [24].

#### 4. Conclusion

PCP could be effectively degraded by Mont-TiO<sub>2</sub> and Mont-Bi-Ti nanocomposites in aqueous solution under UV light. In this study, the experimental results showed that the characterization of these nanocomposites by XRD, BET, SEM and FTIR analysis confirmed the intercalation of TiO<sub>2</sub> and Bi<sub>2</sub>O<sub>3</sub> in montmorillonite. The results show that PCP photodegradation efficiency which was weak when photolysis and adsorption were carried out. The photocatalysts Mont-TiO<sub>2</sub> and Mont-Bi-Ti were successfully used for photocatalytic degradation of PCP in aqueous media, which proves the high catalytic activity of the photocatalyst and a better degradation obtained in acid medium followed by the pH of the solution and photocatalysts concentration.

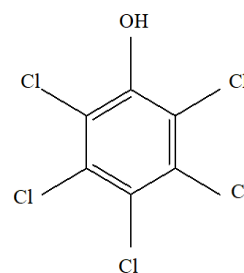


Figure 9. Chemical structure of Pentachlorophenol (PCP).

### Acknowledgments

The author would like to acknowledge the support to the *Laboratoire de Génie Chimique (LGC), Faculté de Technologie, Université Blida 1*.

### References

- [1] Khuzwayo, Z., Chirwa, E.M.N. (2017). The impact of alkali metal halide electron donor complexes in the photocatalytic degradation of pentachlorophenol. *Journal of Hazardous Materials*, 321, 424–431. DOI: 10.1016/j.jhazmat.2016.08.069
- [2] Govindan, K., Murugesan, S., Maruthamuthu, P. (2013). Photocatalytic degradation of pentachlorophenol in aqueous solution by visible light sensitive NF-codoped TiO<sub>2</sub> photocatalyst. *Materials Research Bulletin*, 48(5), 1913–1919. DOI: 10.1016/j.materresbull.2013.01.047
- [3] Gunlazuardi, J., Lindu, W.A. (2005). Photocatalytic degradation of pentachlorophenol in aqueous solution employing immobilized TiO<sub>2</sub> supported on titanium metal. *Journal of Photochemistry and Photobiology A: Chemistry*, 173(1), 51–55. DOI: 10.1016/j.jphotochem.2005.01.002
- [4] Houari, M., Saidi, M., Tabet, D., Pichat, P., Khalaf, H. (2005). The removal of 4-chlorophenol and dichloroacetic acid in water using Ti-, Zr- and Ti/Zr-pillared bentonites as photocatalyst. *American Journal of Applied Sciences*, 2(7), 1136–1140. DOI: 10.3844/ajassp.2005.1136.1140
- [5] Luo, Y., Li, M., Hu, G., Tang, T., Wen, J., Li, X., Wang, L. (2018). Enhanced photocatalytic activity of sulfur-doped graphene quantum dots decorated with TiO<sub>2</sub> nanocomposites. *Materials Research Bulletin*, 97, 428–435. DOI: 10.1016/j.materresbull.2017.09.038
- [6] Patil, S.P., Bethi, B., Sonawane, G.H., Shrivastava, V.S., Sonawane, S. (2016). Efficient adsorption and photocatalytic degradation of Rhodamine B dye over Bi<sub>2</sub>O<sub>3</sub>-bentonite nanocomposites: A kinetic study. *Journal of Industrial and Engineering Chemistry*, 34, 356–363. DOI: 10.1016/j.jiec.2015.12.002
- [7] Meshram, S., Limaye, R., Ghodke, S., Nigam, S., Sonawane, S., Chikate, R. (2011). Continuous flow photocatalytic reactor using ZnO-bentonite nanocomposite for degradation of phenol. *Chemical Engineering Journal*, 172(2), 1008–1015. DOI: 10.1016/j.cej.2011.07.015
- [8] Riaz, U., Ashraf, S.M., Ruhela, A. (2015). Catalytic degradation of orange G under microwave irradiation with a novel nanohybrid catalyst. *Journal of Environmental Chemical Engineering*, 3(1), 20–29. DOI: 10.1016/j.jece.2014.06.010
- [9] Hamane, D., Arous, O., Kaouah, F., Trari, M., Kerdjoudj, H., Bendjama, Z. (2015). Adsorption/photo-electrodialysis combination system for Pb<sup>2+</sup> removal using bentonite/membrane/semiconductor. *Journal of Environmental Chemical Engineering*, 3(1), 60–69. DOI: 10.1016/j.jece.2014.11.003
- [10] Madhusudan Reddy, K., Baruwati, B., Jayalakshmi, M., Mohan Rao, M., Manorama, S.V. (2005). S-, N- and C-doped titanium dioxide nanoparticles: Synthesis, characterization and redox charge transfer study. *Journal of Solid State Chemistry*, 178(11), 3352–3358. DOI: 10.1016/j.jssc.2005.08.016
- [11] Kaur, S., Singh, V. (2007). Visible light induced sonophotocatalytic degradation of Reactive Red dye 198 using dye sensitized TiO<sub>2</sub>. *Ultrasonics Sonochemistry*, 14(5), 531–537. DOI: 10.1016/j.ultsonch.2006.09.015
- [12] Khalfaoui-Boutoumi, N., Boutoumi, H., Khalaf, H., David, B. (2013). Synthesis and characterization of TiO<sub>2</sub>-Montmorillonite / Polythiophene-SDS nanocomposites: Application in the sonophotocatalytic degradation of rhodamine 6G. *Applied Clay Science*, 80-81, 56–62. DOI: 10.1016/j.clay.2013.06.005
- [13] Bessekhoud, Y., Robert, D., Weber, J.-V. (2005). Photocatalytic activity of Cu<sub>2</sub>O/TiO<sub>2</sub>, Bi<sub>2</sub>O<sub>3</sub>/TiO<sub>2</sub> and ZnMn<sub>2</sub>O<sub>4</sub>/TiO<sub>2</sub> heterojunctions. *Catalysis Today*, 101(3-4), 315–321. DOI: 10.1016/j.cattod.2005.03.038
- [14] Bessekhoud, Y., Chaoui, N., Trzpit, M., Ghazzal, N., Robert, D., Weber, J.V. (2006). UV-vis versus visible degradation of Acid Orange II in a coupled CdS/TiO<sub>2</sub> semiconductors suspension. *Journal of Photochemistry and Photobiology A: Chemistry*, 183(1), 218–224. DOI: 10.1016/j.jphotochem.2006.03.025
- [15] Brahimi, R., Bessekhoud, Y., Bouguelia, A., Trari, M. (2007). CuAlO<sub>2</sub>/TiO<sub>2</sub> heterojunction applied to visible light H<sub>2</sub> production. *Journal of Photochemistry and Photobiology A: Chemistry*, 186(2), 242–247. DOI: 10.1016/j.jphotochem.2006.08.013
- [16] Brahimi, R., Bessekhoud, Y., Bouguelia, A., Trari, M. (2008). Improvement of eosin visible light degradation using PbS-sensitized TiO<sub>2</sub>. *Journal of Photochemistry and Photobiology A: Chemistry*, 194(2), 173–180. DOI: 10.1016/j.jphotochem.2007.08.008



- [17] Bessekhoud, Y., Brahimi, R., Hamdini, F., Trari, M. (2012). Cu<sub>2</sub>S/TiO<sub>2</sub> heterojunction applied to visible light Orange II degradation. *Journal of Photochemistry and Photobiology A: Chemistry*, 248, 15–23. DOI: 10.1016/j.solener.2010.03.024
- [18] Brahimi, R., Bessekhoud, Y., Nasrallah, N., Trari, M. (2012). Visible light CrO<sub>4</sub><sup>2-</sup> reduction using the new CuAlO<sub>2</sub>/CdS heterosystem. *Journal of Hazardous Materials*, 219-220, 19–25. DOI: 10.1016/j.jhazmat.2012.03.011
- [19] Li, L., Huang, X., Zhang, J., Zhang, W., Ma, F., Xiao, Z., Gai, S., Wang, D., Li, N. (2015). Multi-layer three-dimensionally ordered bismuth trioxide/titanium dioxide nanocomposite: synthesis and enhanced photocatalytic activity. *Journal of Colloid and Interface Science*, 443, 13–22. DOI: 10.1016/j.jcis.2014.11.062
- [20] Liu, Y., Xin, F., Wang, F., Luo, S., Yin, X. (2010). Synthesis, characterization, and activities of visible light-driven Bi<sub>2</sub>O<sub>3</sub>-TiO<sub>2</sub> composite photocatalysts. *Journal of Alloys and Compounds*, 498(2), 179–184. DOI: 10.1016/j.jallcom.2010.03.151
- [21] Juan, Y., Jian-Tong, L., Juan, M. (2011). Visible light photocatalytic performance of Bi<sub>2</sub>O<sub>3</sub>/TiO<sub>2</sub> nanocomposite particles. *Chinese Journal of Inorganic Chemistry*, 27(3), 547–555.
- [22] Zou, H., Song, M., Yi, F., Bian, L., Liu, P., Zhang, S. (2016). Simulated-sunlight-activated photocatalysis of Methyl Orange using carbon and lanthanum co-doped Bi<sub>2</sub>O<sub>3</sub>-TiO<sub>2</sub> composite. *Journal of Alloys and Compounds*, 680, 54–59. DOI: 10.1016/j.jallcom.2016.04.094
- [23] Rongan, H., Haijuan, L., Huimin, L., Difa, X., Liuyang, Z. (2020). S-scheme photocatalyst Bi<sub>2</sub>O<sub>3</sub>/TiO<sub>2</sub> nanofiber with improved photocatalytic performance. *Journal of Materials Science & Technology*, 52, 145–151. DOI: 10.1016/j.jmst.2020.03.027
- [24] Kargar, F., Bemani, A., Sayadi, M.H., Ahmadpour, N. (2021). Synthesis of modified beta bismuth oxide by titanium oxide and highly efficient solar photocatalytic properties on hydroxychloroquine degradation and pathways. *Journal of Photochemistry and Photobiology A: Chemistry*, 419, 113453. DOI: 10.1016/j.jphotochem.2021.113
- [25] Khalaf, H., Bouras, O., Perrichon, V. (1997). Synthesis and characterization of Al-pillared and cationic surfactant modified Al-pillared Algerian bentonite. *Microporous Materials*, 8(3), 141–150. DOI: 10.1016/S0927-6513(96)00079-X
- [26] Damardji, B., Khalaf, H., Duclaux, L., David, B. (2009). Preparation of TiO<sub>2</sub>-pillared montmorillonite as photocatalyst Part I. Microwave calcination, characterisation, and adsorption of a textile azo dye. *Applied Clay Science*, 44(3-4), 201–205. DOI: 10.1016/j.clay.2008.12.010
- [27] Pichat, P., Khalaf, H., Tabet, D., Houari, M., Saidi, M. (2005). Ti-montmorillonite as photocatalyst to remove 4-chlorophenol in water and methanol in air. *Environmental Chemistry Letters*, 2(4), 191–194. DOI: 10.1007/s10311-004-0090-7
- [28] Damardji, B., Khalaf, H., Duclaux, L., David, B. (2009). Preparation of TiO<sub>2</sub>-pillared montmorillonite as photocatalyst Part II: Photocatalytic degradation of a textile azo dye. *Applied Clay Science*, 45(1-2), 98–104. DOI: 10.1016/j.clay.2009.04.002
- [29] Sing, K.S. (1985). Reporting physisorption data for gas/solid systems with special reference to the determination of surface area and porosity (Recommendations 1984). *Pure and Applied Chemistry*, 57(4), 603-619. DOI: 10.1351/pac198557040603
- [30] Boukhatem, H., Khalaf, H., Djouadi, L., Gonzalez, F.V., Navarro, R.M., Santaballa, J.A., Canle, M. (2017). Photocatalytic activity of mont-La (6%)-Cu<sub>0.6</sub>Cd<sub>0.4</sub>S catalyst for phenol degradation under near UV visible light irradiation. *Applied Catalysis B: Environmental*, 211, 114–125. DOI: 10.1016/j.apcatb.2017.03.074
- [31] Hadj Bachir, D., Khalaf, H., Ferroukhi, S., Boutoumi, Y., Schnee, J., Gaigneaux, E. (2020). Preparation and characterization of TiO<sub>2</sub> pillared clay: effect of palladium and photosensitizer on photocatalytic activity. *Research Journal of Chemistry and Environment*, 24(3), 60-73.
- [32] Castillo, H.L.D., Grange, P. (1993). Preparation and catalytic activity of titanium pillared montmorillonite. *Applied Catalysis A: General*, 103(1), 23–34. DOI: 10.1016/0926-860X(93)85170-T
- [33] Ding, X., An, T., Li, G., Zhang, S., Chen, J., Yuan, J., Zhao, H., Chen, H., Sheng, G., Fu, J. (2008). Preparation and characterization of hydrophobic TiO<sub>2</sub> pillared clay: The effect of acid hydrolysis catalyst and doped Pt amount on photocatalytic activity. *Journal of Colloid and Interface Science*, 320(2), 501–507. DOI: 10.1016/j.jcis.2007.12.042

- [34] Labib, I., Boutoumi, H., Khalaf, H. (2020). Synergistic Effect of Microwave Calcination and Sonophotocatalytic Activity of TiO<sub>2</sub>-Montmorillonite on The Degradation of Direct Yellow 106 and Disperse Violet 1. *Bulletin of Chemical Reaction Engineering & Catalysis*, 15 (2), 304–318. DOI: 10.9767/bcrec.15.2.6999.304-318
- [35] Bessekhoud, Y., Mohammedi, M., Trari, M. (2002). Hydrogen photoproduction from hydrogen sulfide on Bi<sub>2</sub>S<sub>3</sub> catalyst. *Solar Energy Materials and Solar Cells*, 73(3), 339–350. DOI: 10.1016/S0927-0248(01)00218-5
- [36] Xiao, J., Peng, T., Dai, K., Zan, L., Peng, Z. (2007). Hydrothermal synthesis, characterization and its photoactivity of CdS/Reactorite nanocomposites. *Journal of Solid State Chemistry*, 180(11), 3188–3195. DOI: 10.1016/j.jssc.2007.09.009
- [37] Dubey, N., Rayalu, S.S., Labhsetwar, N.K., Naidu, R.R., Chatti, R.V., Devotta, S. (2006). Photocatalytic properties of zeolite-based materials for the photoreduction of methyl orange. *Applied Catalysis A: General*, 303(2), 152–157. DOI: 10.1016/j.apcata.2006.01.043
- [38] Natarajan, T.S., Natarajan, K., Bajaj, H.C., Tayade, R.J. (2013). Enhanced photocatalytic activity of bismuth-doped TiO<sub>2</sub> nanotubes under direct sunlight irradiation for degradation of Rhodamine B dye. *Journal of Nanoparticle Research*, 15(5), 1669. DOI: 10.1007/s11051-013-1669-3
- [39] Chiou, C.-H., Wu, C.-Y., Juang, R.-S. (2008). Photocatalytic degradation of phenol and m-nitrophenol using irradiated TiO<sub>2</sub> in aqueous solutions. *Separation and Purification Technology*, 62(3), 559–564. DOI: 10.1016/j.seppur.2008.03.009
- [40] Dougna, A.A., Gombert, B., Kodom, T., Djaneye-Boundjou, G., Boukari, S.O.B., Leitner, N.K.V., Bawa, L.M. (2015). Photocatalytic removal of phenol using titanium dioxide deposited on different substrates: Effect of inorganic oxidants. *Journal of Photochemistry and Photobiology A: Chemistry*, 305, 67–77. DOI: 10.1016/j.jphotochem.2015.02.012
- [41] Houndedjihou, D., Kodom, T., Dougna, A.A., Tchakala, I., Djaneye-Boundjou, G., Bawa, L.M. (2018). Oxidation of Catechol and Hydroquinone in Aqueous Media by Heterogeneous Photocatalysis Using Thin Layer of TiO<sub>2</sub> P25. *Chemical Science International Journal*, 24(2), 1–10. DOI: 10.9734/CSJI/2018/44176
- [42] Pelentridou, K., Stathatos, E., Karasali, H., Lianos, P. (2009). Photodegradation of the herbicide azimsulfuron using nanocrystalline titania films as photocatalyst and low intensity black light radiation or simulated solar radiation as excitation source. *Journal of Hazardous Materials*, 163(2-3), 756-760. DOI: 10.1016/j.jhazmat.2008.07.023
- [43] Poullos, I., Tsachpinis, I. (1999). Photodegradation of the textile dye Reactive Black 5 in the presence of semiconducting oxides. *Journal of Chemical Technology & Biotechnology: International Research in Process, Environmental & Clean Technology*, 74(4), 349-357. DOI: 10.1002/(SICI)1097-4660(199904)74:4<349::AID-JCTB5>3.0.CO;2-7
- [44] Dong, S., Xia, L., Chen, X., Cui, L., Zhu, W., Lu, Z., Sun, J., Fan, M. (2021). Interfacial and electronic band structure optimization for the adsorption and visible-light photocatalytic activity of macroscopic ZnSnO<sub>3</sub>/graphene aerogel. *Composites Part B: Engineering*, 215, 108765. DOI: 10.1016/j.compositesb.2021.108765
- [45] Sayadi, M.H., Ahmadpour, N., Homaeigohar, S. (2021). Photocatalytic and Antibacterial Properties of Ag-CuFe<sub>2</sub>O<sub>4</sub>@WO<sub>3</sub> Magnetic Nanocomposite. *Nanomaterials*, 11(2), 298. DOI: 10.3390/nano11020298